ANTICANCER RESEARCH *38*: 3375-3385 (2018)
doi:10.21873/anticanres.12604

Broad-spectrum Preclinical Antitumor Activity of Eribulin (Halaven®): Combination with Anticancer Agents of Differing Mechanisms

MAKOTO ASANO[1], JUNJI MATSUI[1], MURRAY J. TOWLE[2], JIAYI WU[3], SHARON MCGONIGLE[3], MARC HILLAIRET DE BOISFERON[4], TOSHIMITSU UENAKA[5], KENICHI NOMOTO[6] and BRUCE A. LITTLEFIELD[2]

[1]*Oncology Business Group, Eisai Co., Ltd., Tsukuba, Japan;*
[2]*Oncology Business Group, Eisai Inc., Andover, MA, U.S.A.;*
[3]*Neurology Business Group, Eisai Inc., Andover, MA, U.S.A.;*
[4]*Oncodesign, Dijon, France;*
[5]*Morphotek, Exton, PA, U.S.A.;*
[6]*Oncology Business Group, Eisai Inc., Woodcliff Lake, NJ, U.S.A.*

Abstract. *Background: Eribulin is used in many countries to treat patients with advanced breast cancer or liposarcoma and exerts in vivo anticancer activity under monotherapy conditions against various human tumor xenograft models. Here, eribulin in combination with mechanistically different anticancer agents was evaluated. Materials and Methods: Eribulin was combined with cytotoxic agents (capecitabine, carboplatin, cisplatin, doxorubicin, gemcitabine) or targeted agents (bevacizumab, BKM-120, E7449, erlotinib, everolimus, lenvatinib, palbociclib) in tumor xenograft models of breast cancer, melanoma, non-small cell lung cancer (NSCLC), and ovarian cancer. Results: Across nearly all models, eribulin with either cytotoxic or targeted agents demonstrated combination activity, defined as the activity demonstrably greater than that of either agent alone. Combination activity was absent only with doxorubicin (MDA-MB-435 model) and with lenvatinib (NCI-H1975 model), both of which responded to the agents as monotherapy. Conclusion: Eribulin has combination activity with multiple agents from different mechanistic classes in several human cancer models, including breast, NSCLC, ovarian, and melanoma.*

Correspondence to: Bruce A. Littlefield, Ph.D., Eisai Inc., 4 Corporate Drive, Andover, MA, 01810, U.S.A. Tel: +1 9788374727, e-mail: bruce_littlefield@eisai.com

Key Words: Eribulin, E7389, NSC 707389, preclinical combinations, xenograft tumor models, chemotherapy, targeted agents.

Eribulin, as its salt form eribulin mesylate (Halaven®), is in clinical use in many countries worldwide for the treatment of certain patients with advanced or metastatic breast cancer or advanced liposarcoma. As a mechanistically unique microtubule dynamics inhibitor (1-3), eribulin exerts its cytotoxic anticancer effects by prevention of normal mitotic spindle formation, induction of irreversible mitotic blockade, and cancer cell death *via* apoptosis (1-6). Recent studies have identified additional effects of eribulin on tumor biology that extend beyond its antimitotic mechanism, including vascular remodeling that results in increased tumor perfusion and reduced tumor core hypoxia (7), and reversal of epithelial-to-mesenchymal transition that results in reduced cell migratory and invasive capacities and reduced seeding of lung metastases in experimental models of metastasis (8). The breadth and unexpected nature of these additional nonmitotic effects of eribulin have led to the hypothesis that eribulin may interact with additional cellular signaling pathways beyond those involved in regulating mitosis. This, in turn, suggests the possibility that eribulin might be effectively combined with cancer drugs from a variety of mechanistic classes. To address this possibility, we extended our previous preclinical *in vivo* evaluations of eribulin under monotherapy conditions (9) to explore *in vivo* activity of eribulin when combined with other cytotoxic and so-called "targeted" anticancer agents. Our results support the concept that eribulin can be favorably combined with a broad set of anticancer agents from widely diverse mechanistic classes, consistent with its effects on tumor biology beyond purely antimitotic activities.

Materials and Methods

Test agents. Eribulin was synthesized by Eisai Laboratories as described elsewhere (10), and was used in the current studies as its mesylate salt, eribulin mesylate (salt form used in clinical formulation Halaven®). Everolimus, lenvatinib, and E7449 were also synthesized by Eisai Laboratories. Bevacizumab was obtained from Genentech (South San Francisco, CA, USA), BKM-120 was from MedChemExpress (Monmouth Junction, NJ, USA), and carboplatin and cisplatin were both from Bristol-Myers Squibb (New York, NY, USA). Capecitabine was obtained as its clinical formulation Xeloda® from Roche Laboratories (New York, NY, USA), while doxorubicin was from Bedford Laboratories (now Hikma/West-Ward Pharmaceuticals; Eatontown, NJ, USA). Erlotinib and gemcitabine were obtained as their clinical formulations, Tarceva® and Gemzar®, from OSI Pharmaceuticals (now Astellas; Northbrook, IL, USA) and Eli Lilly (Indianapolis, IN, USA), respectively. Palbociclib was obtained from Selleckchem (Euromedex, Souffelweyersheim, France).

Human cancer cell lines and tumor xenograft models. All studies using laboratory animals were approved by the appropriate Institutional Animal Care and Use Committees of Eisai Inc.'s Andover, Massachusetts Laboratories (USA), Eisai Co., Ltd.'s Tsukuba Research Laboratories (Tsukuba, Ibaraki, Japan), the Southern Research Institute (Birmingham, AL, USA), or Oncodesign (Dijon, France), and adhered to all applicable laws and guidelines for the humane care and use of laboratory animals. *In vivo* anticancer effects of eribulin were evaluated in immunocompromised mice using subcutaneous (*s.c.*) tumor xenograft models of the following human cancer types: triple-negative breast cancer (TNBC; HCC70, HCC1187, HCC1806, MDA-MB-231, MDA-MB-436, MX-1); estrogen receptor-positive (ER+) breast cancer (MCF-7); human epidermal growth factor receptor 2 (HER2)-positive breast cancer (UISO-BCA-1); ER+/progesterone receptor-positive (PR+)/HER2-negative patient-derived xenograft (PDX) breast cancer (OD-BRE-0192, OD-BRE-0745); non-small cell lung cancer (NSCLC; A549, NCI-H322M, NCI-H522, NCI-H1975, NCI-H1993, PC-9), ovarian cancer (A2780, A2780cis, SK-OV-3), and melanoma (A375, MDA-MB-435).

The NCI-H522, MDA-MB-436, A375, HCC70, HCC1187, HCC1806, MCF7, NCI-H1975, NCI H1993, and SK-OV-3 cell lines were obtained from the American Type Culture Collection (Manassas, VA, USA). The MDA-MB-435, MX-1, and NCI-H322M cell lines were obtained from the NCI Division of Cancer Treatment Tumor Repository (Frederick, MD, USA). The A2780, A2780cis, and A549 cell lines were obtained from DS Pharma Biomedical (Osaka, Japan). The PC-9 cell line was obtained from ImmunoBiological Laboratories (Gunma, Japan). The UISO-BCA-1 cell line was obtained from Southern Research Institute (now Southern Research; Birmingham, AL, USA). All cell lines were grown according to repository-recommended conditions.

The OD-BRE-0192 PDX model (ER+/PR+/HER2−) was generated from a clinical sample obtained from a 45-year-old female with luminal B invasive lobular breast carcinoma with the presence of lymph node metastases. The patient was a poor responder to prior therapies, including epirubicin, 5-fluorouracil, cyclophosphamide, taxotere, paclitaxel, bevacizumab, and gemcitabine. The OD-BRE-0745 PDX model (ER+/PR+/HER2−) was generated from a clinical sample obtained from a 78-year-old female diagnosed with luminal B poorly differentiated infiltrating ductal adenocarcinoma with lymph node metastases. The patient had not received any chemotherapy or radiotherapy prior to surgery. For generation of OD-BRE-0192 and OD-BRE-0745 PDX models, all clinical samples were collected under written informed consent (according to the Declaration of Helsinki) and a declaration for commercial use of the samples from the Consultative Committee for the Protection of Persons in Biomedical Research (CCPPRB) of Dijon University Hospital under authorization by the French Ministry of Higher Education, Research and Innovation for human tissue collection, storage, and redistribution (CSP articles L 1243-3, L 1243-4, and L 1245-5). PDX tumors were passaged by serial transplantation in immunocompromised mice.

We previously reported eribulin activity against MDA-MB-435 cells and xenografts as representative preclinical models of breast cancer (5). Rigorous genetic studies by several groups have now shown that this cell line is of melanoma origin (11). Accordingly, in this report, we adopt the currently accepted identity of MDA-MB-435 as being of melanoma origin.

In all *in vivo* models derived from established human cancer cell lines, *s.c.* human tumor xenografts were generated *via* inoculation of 5- to 8-week-old female nu/nu mice (obtained from either Harlan Sprague Dawley Inc., Indianapolis, IN, USA, or Japan SLC Inc., Shizuoka, Japan [or C.B-17 SCID mice from Charles River Laboratories, Wilmington, MA, USA, for the MDA-MB-436 model]) either with cell suspensions from *in vitro* cell cultures, or with serially passaged 30-40 mg tumor fragments, the latter implanted using 12- or 13-gauge trocar needle insertion. Randomization into treatment groups for subsequent drug administration was performed after all *s.c.* tumors had reached volumes of 75-200 mm^3. Group sizes in each study were between 4-10 mice.

Two PDX models established at Oncodesign, OD-BRE-0192 and OD-BRE-0745, were used for studies of eribulin in combination with palbociclib. PDX model OD-BRE-0192 was used at *in vivo* passage 11 (post-patient surgery). PDX model OD-BRE-0745 was used at *in vivo* passage 5 (post-patient surgery). *In vivo s.c.* PDX models were generated *via* implantation of 5- to 8-week-old female nu/nu mice with serially passaged 30-40 mg tumor fragments. All tumor fragment implantations were performed 24-48 h after whole-body irradiation with a γ-irradiation source (2 Gy, ^{60}Co; BioMEP, Bretenières, France). All mice carrying OD-BRE-0192 and OD-BRE-0745 PDX models for passage, amplification, or experimentation received water continuously supplemented with 2.5 μg/ml estradiol. For experiments in both models, treatments started when tumors reached mean volumes of 200-300 mm^3.

Drug administration. All dosing and scheduling information for eribulin combination experiments are summarized in Table I. In many studies, suboptimal doses of eribulin, the combination agent being tested, or both agents were selected to visualize combination effects that might otherwise have been masked by more dominant effects of the agents at higher dose levels. Thus, discussion of results in this article does not address apparent comparative activities of eribulin and combination agents when given under monotherapy conditions.

Measurements and evaluation of results. The maximum tolerated dose (MTD), for monotherapy and combination therapy was defined as the highest dose level inducing no more than (i) 20% loss of mean group body weight, reversible upon cessation of dosing, or (ii) 10% lethality in a group that otherwise showed less

Table I. *Summary of eribulin activity in combination with cytotoxic or targeted anticancer agents.*

	Combination agent					Eribulin, *i.v.*		
Agent	Target and mechanism	Model	Tumor type	Dose, mg/kg	Schedule	Dose, mg/kg	Schedule	Combination activity
Cytotoxic agents								
Capecitabine, *p.o.*	TS (5-FU prodrug)	MX-1	TNBC	500	*q1dx14*	0.2-0.4	*q4dx4*	+
		UISO-BCA-1	HER2+ BC	500	*q1dx14*	0.2-0.4	*q4dx4*	+
Carboplatin, *i.v.*	Platinum-based, DNA damage	HCC1806	TNBC	80	*q1dx1*	0.3	*q7dx2*	+
		MX-1	TNBC	80	*q1dx1*	0.3	*q7dx2*	+
		A2780	Ovary	80	*q1dx1*	0.3	*q7dx2*	+
		A2780cis	Ovary, cisPt resistant	80	*q1dx1*	0.3	*q7dx2*	–
Cisplatin, *i.v.*	Platinum-based, DNA damage	HCC1806	TNBC	8	*q1dx1*	0.3	*q7dx2*	+
		MX-1	TNBC	8	*q1dx1*	0.3	*q7dx2*	+
		A2780	Ovary	8	*q1dx1*	0.3	*q7dx2*	+
		A2780cis	Ovary, cisPt resistant	8	*q1dx1*	0.3	*q7dx2*	–
Doxorubicin, *i.v.*	DNA intercalator, topoisomerase II	MDA-MB-435	Melanoma	5.36	*q4dx3*	0.12-0.4	*q4dx3*	–
Gemcitabine, *i.v.*	RR, DNA chain terminator	NCI-H522	NSCLC	120	*q3dx4*	0.12-0.4	*q4dx3*	+
Targeted agents								
Bevacizumab, *i.v.*	VEGF	MDA-MB-231	TNBC	10	*q3dx2 (x2)*	1.5-2.5	*q7dx2*	+
		SK-OV-3	Ovary	10	*q3dx2 (x2)*	3.5	*q7dx2*	+
BKM-120, *p.o.*	PI3K	NCI-H1993	NSCLC	20	*q1dx14*	1.5	*q7dx2*	+
		PC-9	NSCLC	20	*q1dx12*	1.5	*q7dx2*	+
		A549	NSCLC	20	*q1dx14*	1.5	*q7dx2*	+
Erlotinib, *p.o.*	EGFR	NCI-H322	NSCLC	50-75	*q1dx3 (x4)*	0.8	*q4dx4*	+
Everolimus, *p.o.*	mTOR	MX-1	TNBC	20-40	*q1dx16*	0.4	*q4dx4*	+
		MCF-7	ER+ BC	10	*q1dx14*	1.5	*q7dx2*	+
E7449, *p.o.*	PARP/tankyrase	MDA-MB-436	TNBC	60	*q1dx28*	0.4-1.6	*q4dx4*	+
Lenvatinib, *p.o.*	VEGFR/ FGFR/PDGFRα/ RET/KIT	A375	Melanoma	15	*q1dx14*	0.05-3.0	*q7dx2*	+
		NCI-H1993	NSCLC	10	*q1dx12*	1.5	*q7dx2*	+
		PC-9	NSCLC	10	*q1dx12*	1.5	*q7dx2*	+
		HCC1806	TNBC	10	*q1dx14*	1.5	*q7dx2*	+
		HCC70	TNBC	10	*q1dx14*	1.5	*q7dx2*	+
		HCC1187	TNBC	10	*q1dx14*	1.5	*q7dx2*	+
		MCF-7	ER+ BC	10	*q1dx14*	1.5	*q7dx2*	+
		A549	NSCLC	10	*q1dx14*	1.5	*q7dx2*	+
		NCI-H1975	NSCLC	10	*q1dx14*	1.5	*q7dx2*	–
Palbociclib, *p.o.*	CDK4/6	OD-BRE-0192 (PDX)	ER+/HR+/HER2– BC	150	*q1dx5 (x3)*	0.25	*q7dx3*	+
		OD-BRE-0745 (PDX)	ER+/HR+/HER2– BC	75	*q1dx5 (x4)**	0.25	*q7dx4**	+

5-FU, 5-Fluorouracil; BC, breast cancer; CDK, cyclin-dependent kinase; cisPt, cisplatin; DNA, deoxyribonucleic acid; EGFR, epidermal growth factor receptor; ER+, estrogen receptor-positive; FGFR, fibroblast growth factor receptor; HER2+/–, human epidermal growth factor receptor 2-positive/ -negative; *i.v.*, intravenous; KIT, kit proto-oncogene, also known as CD117 or stem cell factor receptor; mTOR, mammalian target of rapamycin; NSCLC, non-small cell lung cancer; PARP, poly(ADP-ribose) polymerase; PDGFRα, platelet-derived growth factor receptor α; PDX, patient-derived xenograft; PI3K, phosphoinositide-3-kinase; *p.o.*, *per os*; RET, ret proto-oncogene; RR, ribonucleotide reductase; TNBC, triple-negative breast cancer; TS, thymidylate synthase; VEGF, vascular endothelial growth factor; VEGFR, vascular endothelial growth factor receptor. *In the OD-BRE-0745 PDX model, a fourth full weekly cycle of administrations for all treatment groups was included, starting 8 days after the final palbociclib dose from the first three weekly cycles. +: Combination activity observed; –: no combination activity observed.

than 20% reversible mean group body-weight loss. All data presented here represent results obtained at or below the defined MTD whether for monotherapy or combination therapy. Tumor volumes of *s.c.* xenografts were determined based on caliper measurements and the formula $V=(L\times W^2)/2$, in which L and W refer to the larger (length) and smaller (width) tumor dimensions in mm, respectively. Body weights of mice were measured individually using a tared platform balance on the same days that tumor volume measurements were obtained. Depending on the model or study, antitumor activity was variously defined and

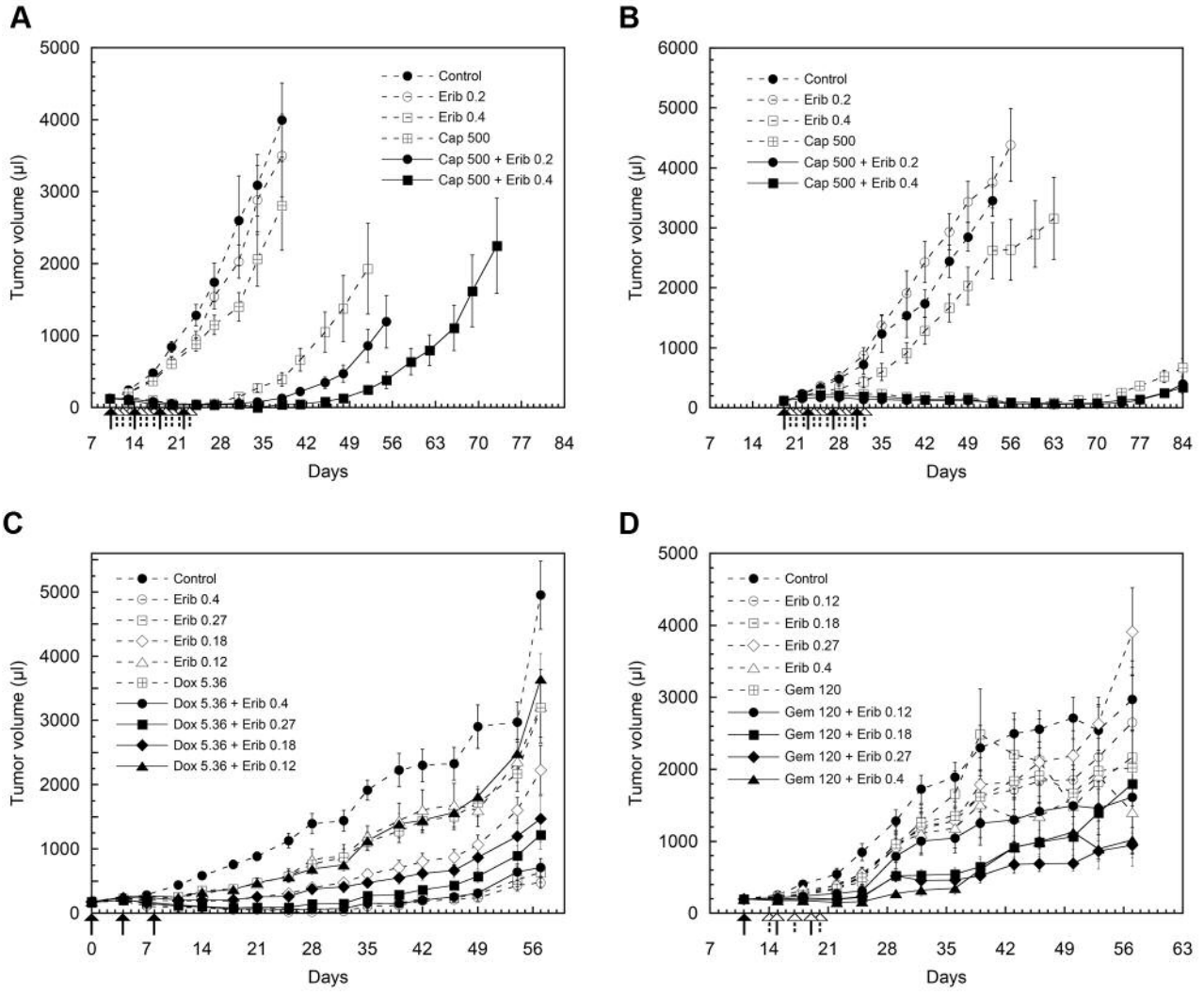

Figure 1. *In vivo combination activity of eribulin (Erib) with cytotoxic agents in human xenograft models of breast cancer, melanoma, and non-small cell lung cancer (NSCLC). A: Eribulin plus capecitabine in the MX-1 triple-negative breast cancer model. B: Eribulin plus capecitabine (Cap) in the UISO-BCA-1 (human epidermal growth factor receptor 2-positive breast cancer model). C: Eribulin plus doxorubicin (Dox) in the MDA-MB-435 melanoma model. D: Eribulin plus gemcitabine (Gem) in NCI-H522 NSCLC model. Data represent mean±SEM. Dose levels (mg/kg) of all agents are as shown in the graphs. Dosing days for drugs are shown with arrows below the x-axes as follows: eribulin alone, open arrows with solid line; combination drug only, open arrows with dotted line; both drugs together, solid arrows with solid line.*

compared between groups as tumor growth rate inhibition, partial or complete tumor regression or, with complete regressions, times to reappearance of tumor regrowth. Combination activity was defined as antitumor activity demonstrably greater than that of either agent alone. This report does not attempt to distinguish between additivity and synergy because such terms are necessarily subjective, can differ between different time points in the same study, and are often used to suggest mechanistic aspects that the current studies were not designed to address. Thus, our use of "combination activity" intentionally includes both situations, with no intended implication as to any mechanisms of interactions resulting in the effects observed.

Results

Combination with cytotoxic agents. Combinations of eribulin with different antimetabolites and a DNA intercalator were evaluated in several human cancer xenograft models. In both the MX-1 and UISO-BCA-1 breast cancer models (Figure 1A and B, respectively), eribulin given on a *q4dx4* schedule showed *in vivo* combination activity with capecitabine given on a *q1dx14* schedule. Interestingly, in the MDA-MB-435 melanoma xenograft model, eribulin given on a *q4dx3* schedule failed to show *in vivo* combination activity with

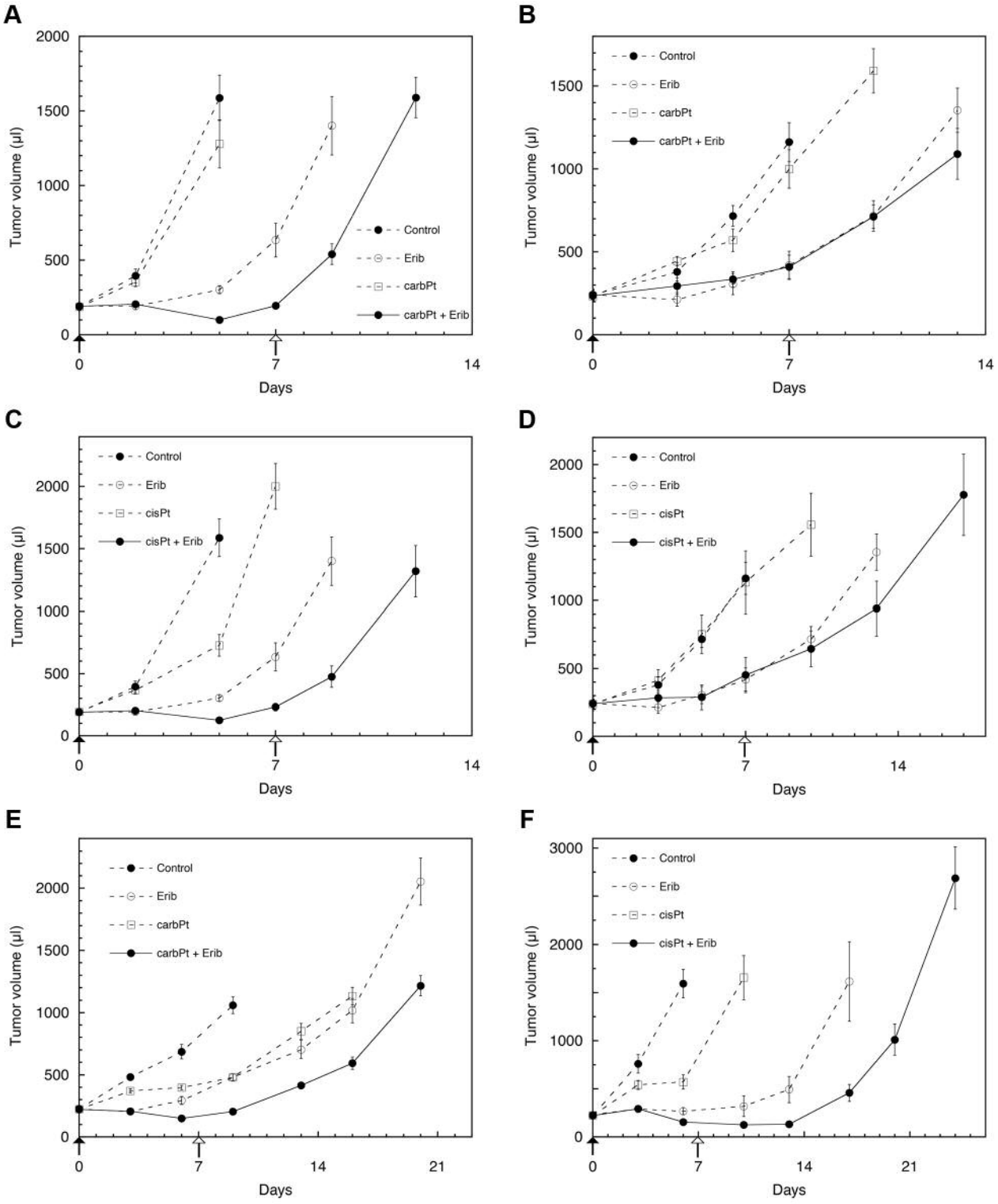

Figure 2. *In vivo combination activity of eribulin with platinum-based cytotoxic agents in human xenograft models of ovarian and breast cancer. A: Eribulin (Erib) plus carboplatin (carbPt) in the A2780 ovarian cancer model. B: Eribulin plus carboplatin in the A2780cis ovarian cancer model. C: Eribulin plus cisplatin (cisPt) in the A2780 ovarian cancer model. D: Eribulin plus cisplatin in the A2780cis ovarian cancer model. E: Eribulin plus carboplatin in the HCC1806 triple-negative breast cancer (TNBC) model. F: Eribulin plus cisplatin in the MX-1 TNBC model. Data represent mean±SEM. Dosing days for drugs are shown with arrows below the x-axes as follows: eribulin alone, open arrows with solid line; combination drug only, open arrows with dotted line; both drugs together, solid arrows with solid line.*

doxorubicin given on a *q4dx3* schedule (Figure 1C), even at the highest tested dose of eribulin. However, in the NCI-H522 NSCLC xenograft model, eribulin given on a *q4dx3* schedule demonstrated *in vivo* combination activity with gemcitabine given on a *q3dx4* schedule (Figure 1D).

Combinations of eribulin with carboplatin and cisplatin were tested in ovarian and breast cancer xenograft models. In the A2780 ovarian cancer model, eribulin given on a *q7dx2* schedule demonstrated *in vivo* combination activity with both carboplatin (Figure 2A) and cisplatin (Figure 2C), each given on a *q1dx1* schedule. As predicted, based on the known resistance of the A2780cis cell line to platinum agents (12), eribulin failed to show combination activity with either carboplatin or cisplatin despite having single-agent activity of its own (Figure 2B and D) using the same doses and schedules as in the cisplatin-sensitive A2780 model.

Carboplatin and cisplatin were also tested as combination agents in two TNBC models. Using the same dosing schedules as in the ovarian models above, *in vivo* combination activity of eribulin with carboplatin was seen in the HCC1806 and MX-1 TNBC models (Figure 2E), while combination activity with cisplatin was observed in the same models (Figure 2F).

Combination with targeted agents. Eribulin was next tested in combination with targeted agents, including bevacizumab, the investigational agent BKM-120 (13), erlotinib, and everolimus. In both the MDA-MB-231 TNBC and SK-OV-3 ovarian cancer xenograft models, eribulin given on a *q7dx2* schedule combined with the monoclonal antibody to vascular endothelial growth factor (VEGF) bevacizumab on a *q3dx2(x2)* schedule showed *in vivo* combination activity (Figure 3A and B, respectively). Eribulin given on a *q7dx2* schedule also showed combination activity with the phosphoinositide-3-kinase (PI3K) inhibitor BKM-120 given on a *q1dx14* schedule in both the NCI-H1993 and A549 NSCLC models (Figure 3C and Table I), or on a *q1dx12* schedule in the PC-9 NSCLC model (Table I). In the NCI-H322M NSCLC xenograft model, eribulin given on a q4dx4 schedule demonstrated *in vivo* combination activity with the epidermal growth factor receptor (EGFR) kinase inhibitor erlotinib given on a *q1dx3(x4)* schedule (Figure 3D). In both the MCF-7 (ER+) and the MX-1 (TNBC) xenograft models, eribulin given on schedules of *q7dx2* and *q4dx4*, respectively, showed *in vivo* combination activity with the mammalian target of rapamycin (mTOR) inhibitor everolimus given on *q1dx14* and *q1dx16* schedules, respectively (Figure 3E and F).

Eribulin was evaluated in combination with the dual poly (ADP-ribose) polymerase (PARP) and tankyrase inhibitor E7449 (14) in a TNBC xenograft model and with the multitargeted tyrosine kinase inhibitor lenvatinib in various xenograft models of melanoma, breast cancer, and NSCLC. Eribulin given on a *q4dx4* schedule demonstrated *in vivo* combination activity with E7449 given on a *q1dx28* schedule in the MDA-MB-436 TNBC xenograft model (Figure 4A). Combination activity of eribulin on a *q7dx2* schedule with lenvatinib on a *q1dx14* schedule (except NCI-H1993 and PC-9 models that received lenvatinib on a *q1dx12* schedule) was observed in eight different xenograft models: A375 melanoma (Figure 4B); a panel of breast cancer models, including TNBC models HCC1806, HCC70, and HCC1187 (Figure 4C and Table I) and ER+ model MCF-7 (Figure 4D); and multiple NSCLC xenograft models, including NCI-H1993, A549, and PC-9 (Figure 4E and Table I).

Finally, eribulin was tested in combination with the selective inhibitor of cyclin-dependent kinase 4/6 (CDK4/6) palbociclib in 2 PDX models of ER+/PR+/HER2− breast cancer derived from separate female patients with luminal B breast cancer subtype. In the OD-BRE-0192 model, eribulin given on a *q7dx3* schedule demonstrated *in vivo* combination activity with palbociclib given on a *q1dx5(x3)* schedule (Figure 5A). Similar combination activity was seen in the OD-BRE-0745 model, which included a fourth weekly cycle of dosing starting 8 days after the last palbociclib dose from the first three cycles (Figure 5B).

Discussion

Previous publications from our laboratories have demonstrated potent cell-based anticancer activity of eribulin against a wide range of human cancer cell types, including sub- or low-nanomolar activity against colon cancer, Ewing's sarcoma, fibrosarcoma, histiocytic lymphoma, leiomyosarcoma, liposarcoma, melanoma, promyelocytic leukemia, prostate cancer, and synovial sarcoma cell lines (5, 15). Other studies from our groups have shown robust *in vivo* activity of eribulin administered as a monotherapy agent against a wide range of human tumor xenograft models, including breast cancer, colon cancer, Ewing's sarcoma, fibrosarcoma, glioblastoma, head and neck cancer, leiomyosarcoma, liposarcoma, melanoma, NSCLC, ovarian cancer, pancreatic cancer, and small cell lung cancer (5, 7, 9, 15). In addition, work by the National Cancer Institute's Pediatric Preclinical Testing Program has reported potent *in vitro* and *in vivo* activity of eribulin against a variety of preclinical pediatric cancer models, including several B- and T-cell leukemias, ependymoma, Ewing's sarcoma, glioblastoma, malignant rhabdoid and Wilms' tumors, medulloblastoma, neuroblastoma, osteosarcoma, and rhabdomyosarcoma (16). These studies of eribulin administered as a single agent have established it as an anticancer agent with potent activity against a broad range of preclinical tumor models representing a variety of solid and blood cancers from both the adult and pediatric settings. The current studies described here extend the monotherapy observations summarized above to additionally establish eribulin as an agent that can be effectively combined with other anticancer agents

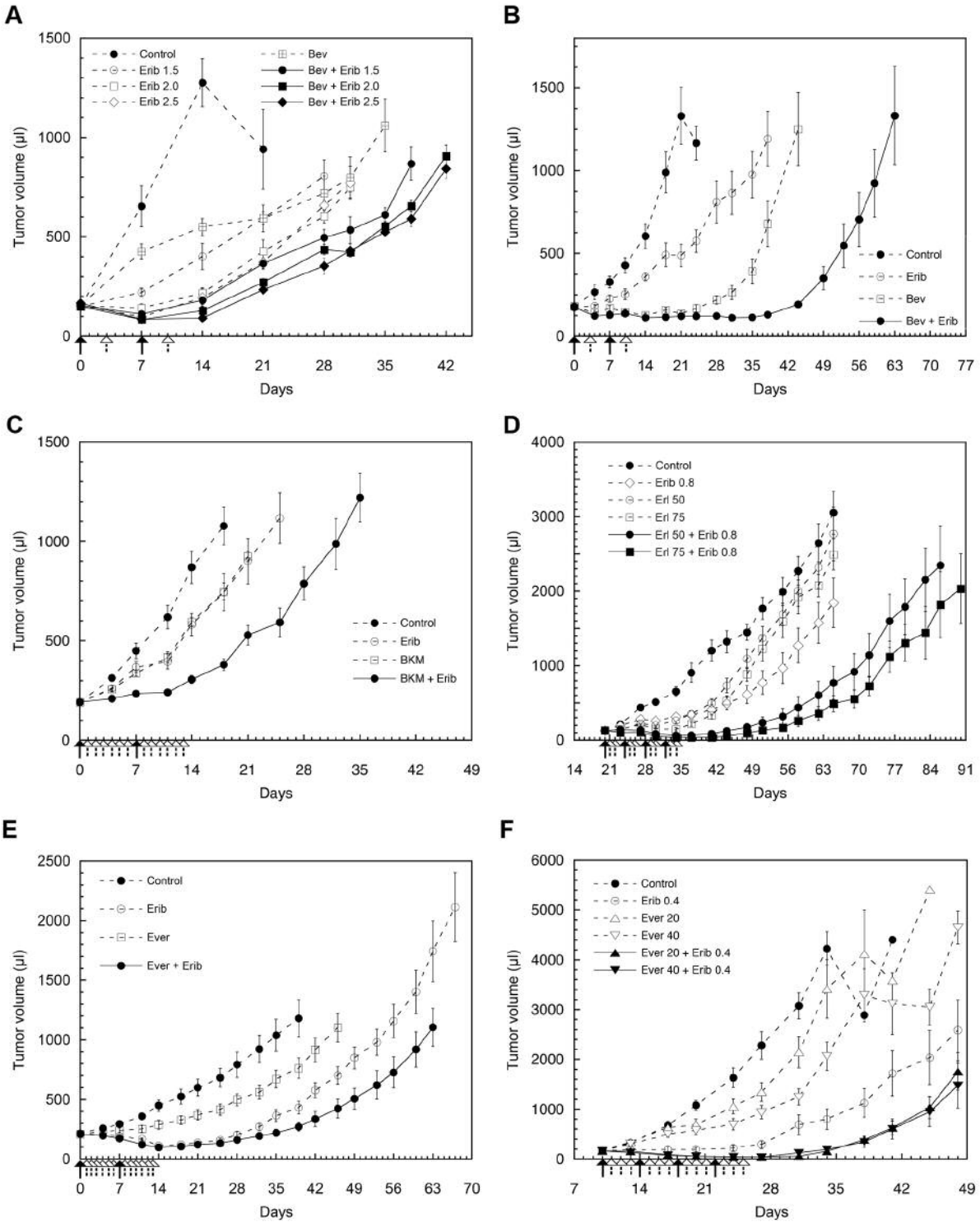

Figure 3. *In vivo combination activity of eribulin with targeted agents in human xenograft models of breast cancer, ovarian cancer, and non-small cell lung cancer (NSCLC). A: Eribulin (Erib) plus bevacizumab (Bev) in the MDA-MB-231 triple-negative breast cancer (TNBC) model. B: Eribulin plus bevacizumab in the SK-OV-3 ovarian cancer model. C: Eribulin plus BKM-120 (BKM) in the NCI-H1993 NSCLC model. D: Eribulin plus erlotinib (Erl) in the NCI-H322M NSCLC model. E: Eribulin plus everolimus in the MCF-7 estrogen receptor-positive breast cancer model. F: Eribulin plus everolimus (Ever) in the MX-1 TNBC model. Data represent mean±SEM. Dose levels (mg/kg) of agents are as shown in the graphs (A, D, and F) (doses used for experiments shown in panels B, C and E can be found in Table I). Dosing days for drugs are shown with arrows below the x-axes as follows: eribulin alone, open arrows with solid line; combination drug only, open arrows with dotted line; both drugs together, solid arrows with solid line.*

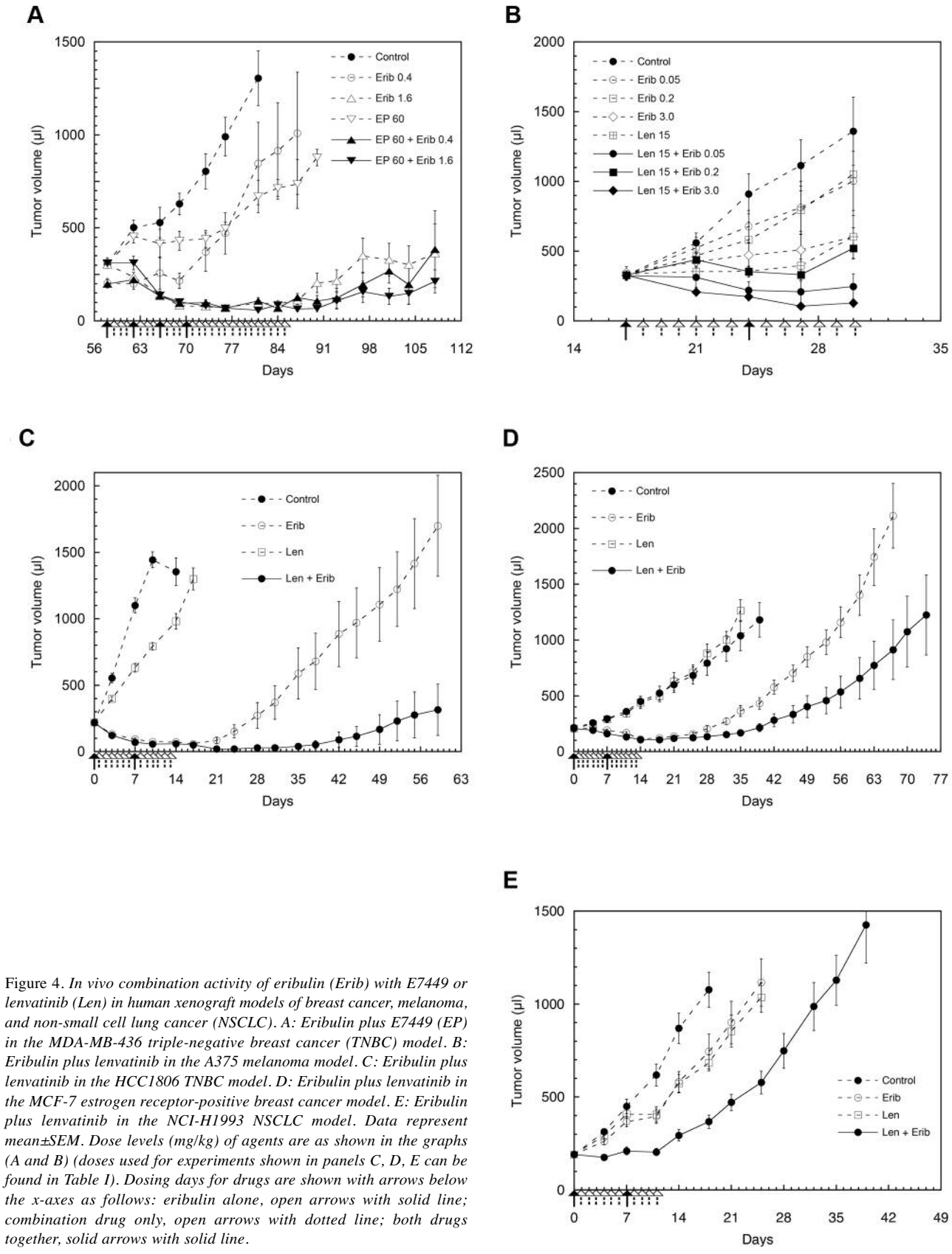

Figure 4. *In vivo combination activity of eribulin (Erib) with E7449 or lenvatinib (Len) in human xenograft models of breast cancer, melanoma, and non-small cell lung cancer (NSCLC). A: Eribulin plus E7449 (EP) in the MDA-MB-436 triple-negative breast cancer (TNBC) model. B: Eribulin plus lenvatinib in the A375 melanoma model. C: Eribulin plus lenvatinib in the HCC1806 TNBC model. D: Eribulin plus lenvatinib in the MCF-7 estrogen receptor-positive breast cancer model. E: Eribulin plus lenvatinib in the NCI-H1993 NSCLC model. Data represent mean±SEM. Dose levels (mg/kg) of agents are as shown in the graphs (A and B) (doses used for experiments shown in panels C, D, E can be found in Table I). Dosing days for drugs are shown with arrows below the x-axes as follows: eribulin alone, open arrows with solid line; combination drug only, open arrows with dotted line; both drugs together, solid arrows with solid line.*

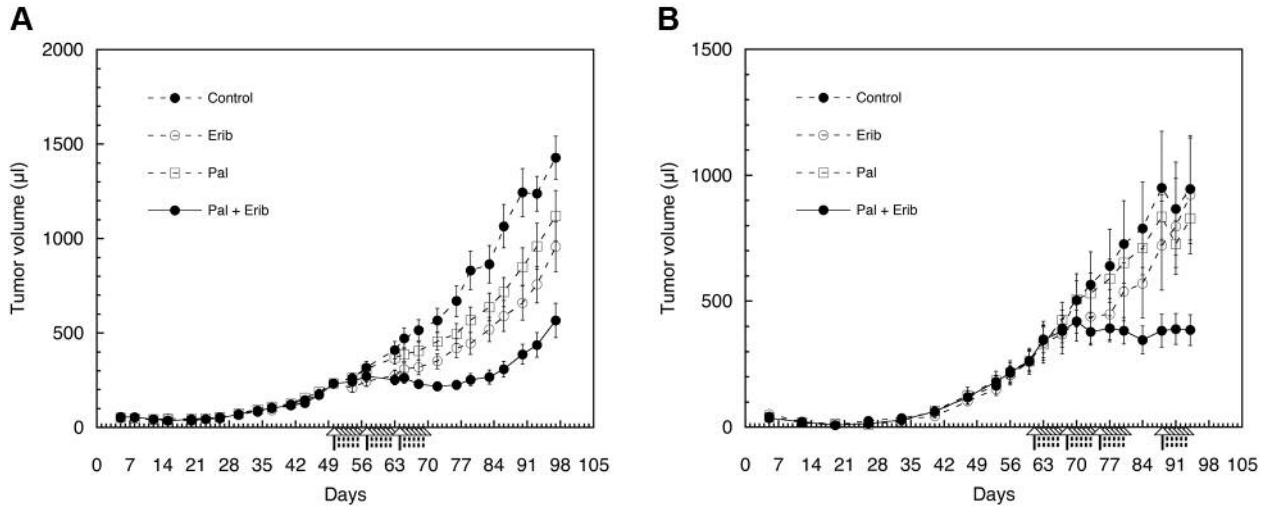

Figure 5. *In vivo combination activity of eribulin (Erib) with palbociclib (Pal) in patient-derived xenograft breast cancer (estrogen receptor-positive/progesterone receptor-positive/human epidermal growth factor receptor 2-positive) models. A: Eribulin plus palbociclib in the OD-BRE-0192 breast cancer model. B: Eribulin plus palbociclib in the OD-BRE-0745 breast cancer model. Data represent mean±SEM. Dosing days for drugs are shown with arrows below the x-axes as follows: eribulin alone, open arrows with solid line; combination drug only, open arrows with dotted line; both drugs together, solid arrows with solid line.*

having widely differing mechanisms of action. Similar to the monotherapy studies, these combination studies encompass preclinical models representing a wide range of different human tumor types.

A summary of results from the present combination studies is presented in Table I. Taken together, four general conclusions are supported by the results of our studies. The first general conclusion concerns the generality with which eribulin exhibited combination activity with other agents: In 32 separate investigations conducted with 12 different agents, using 21 xenograft models representing six different types of human cancer, only four exceptions were seen in which eribulin failed to show positive combination activity with the tested agent. As such, the data presented here are consistent with eribulin being an agent of choice for combining with other drugs in general, regardless of mechanism or tumor type. As for the four exceptions, two represented eribulin combined with either carboplatin or cisplatin in the A2780cis ovarian cancer xenograft model, and were expected based on the known resistance of this model to platinum-based agents (12). A third exception was combining eribulin with the multitargeted tyrosine kinase inhibitor lenvatinib in the NCI-H1975 NSCLC model (Table I). Unexpectedly, in this model, eribulin as monotherapy was more effective at preventing tumor regrowth than when combined with lenvatinib. This apparent antagonism was not seen in eight other melanoma, breast cancer, and NSCLC models using this combination, suggesting that genetic or epigenetic characteristics specific to the NCI-H1975 NSCLC cell line may account for this behavior; further studies will be required to more fully understand this interesting observation. The fourth exception was seen in the MDA-MB-435 melanoma model when combining eribulin with the DNA intercalator and topoisomerase II inhibitor doxorubicin. Oddly, neither activity nor overt antagonism was seen with this combination, even though both agents showed clear activity when given separately as single agents. It is unclear why two active agents could show such a complete lack of interaction when given together. However, we speculate that it may represent a type of cryptic, mechanistic antagonism that we propose calling "exclusionary antagonism" to distinguish it from the typically observable "overt antagonism" in which the activity of two drugs combined is less than the activity of either one alone. In this scenario, the hallmark of exclusionary antagonism would be when a combination of two active agents does not result in reduced activity relative to either agent alone, but rather the actions of one drug preclude the activity of the other drug, and *vice versa*. Which drug blocks the action of the other in individual cells might be dependent on the cell-cycle phase of the cells when first exposed, cell-to-cell variability in drug metabolism or efflux, or other parameters that relate to the myriad of cell-to-cell variations in nonclonal cell populations. Further studies will be required to determine if the exclusionary antagonism hypothesis explains the unexpected lack of interaction between eribulin and doxorubicin in the MDA-MB-435 melanoma model.

The second general conclusion from the current studies is that combination activity of eribulin is manifest with agents from a wide variety of mechanistic categories. Among cytotoxic agents, positive combination activity was seen with inhibitors of nucleotide biosynthesis (capecitabine), DNA synthesis (gemcitabine), and platinum-based DNA-damaging agents. Among targeted agents, combination activity with eribulin was seen with monoclonal antibodies targeting VEGF (bevacizumab), inhibitors of PI3K (BKM-120), EGFR kinase (erlotinib), mTOR (everolimus), and PARP/tankyrase (E7449), a multitargeted tyrosine receptor kinase inhibitor that targets VEGF receptor, fibroblast growth factor receptor, platelet-derived growth factor receptor alpha, KIT and RET (lenvatinib), as well as a CDK4/6 inhibitor (palbociclib). Thus, with the possible exception of doxorubicin discussed in the previous paragraph, the tubulin-based anticancer mechanisms of eribulin do not appear to clash mechanistically with agents from a wide variety of mechanistic classes. Of particular interest is the combination activity of eribulin and the CDK4/6 inhibitor palbociclib observed in 2 ER+/PR+/HER2− breast cancer PDX models, which provides a preclinical foundation for exploring an eribulin plus palbociclib combination strategy in appropriate breast cancer patients.

The third general conclusion from the current studies is that the ability of eribulin to combine with a wide variety of drugs is seen across a broad spectrum of different human tumor types as represented by preclinical human tumor xenografts. In the current studies, combination activity of eribulin with other drugs was seen in models of ER+, HER2+, and TNBC, melanoma, NSCLC, and ovarian cancer. In this regard, the broad spectrum of combination activity of eribulin against several tumor types is reminiscent of the similar breadth of activity seen under monotherapy conditions as described above (5, 7, 9, 15, 16).

The fourth general conclusion from the current studies concerns observations made specifically in breast cancer models. In these studies, combination activity of eribulin with different anticancer agents was consistently seen across three major subtypes of breast cancer, including ER+, HER2+, and TNBC, observations that are consistent with the current clinical use of eribulin for certain patients with advanced or metastatic breast cancer (17).

Additionally, the current studies fill a gap created by reassignment of the MDA-MB-435 model from breast cancer to melanoma (11); our previous reports of the *in vivo* activity of eribulin against this model referred to it using its previous designation as a breast cancer model (5, 9). The current studies showing *in vivo* combination activity of eribulin against ER+ (MCF-7), HER2+ (UISO-BCA-1), and TNBC (HCC70, HCC1187, HCC1806, MDA-MB-231, MDA-MB-436, MX-1) breast cancer models thus remedy the preclinical breast cancer data gap created by reassignment of the MDA-MB-435 model as melanoma.

The results of the current studies support the concept of eribulin as a potential agent of choice for effective chemotherapeutic combinations with cytotoxic and targeted agents from widely differing mechanistic classes, with the important caveats that: (i) human tumor xenograft models may not predict human clinical activity, and (ii) preclinical models using immunocompromised mice cannot capture the full biological complexity of the human tumor microenvironment, including immunological, stromal, vascular, and other aspects. Thus, caution is warranted when extrapolating the current results to potential human therapeutic approaches. Nevertheless, the preclinical evidence presented here documenting broad combination activities of eribulin with multiple agents of differing mechanisms, across a spectrum of tumor types, provides sound justification for continued exploration of new clinical combinations of eribulin with other anticancer agents.

Acknowledgements

The Authors thank Eva Skokanova, Venus Estrada, and Catherine Reardon for their excellent technical assistance with experiments. The Authors are also grateful to Dr. Eli Berdougo of Oxford PharmaGenesis, Newtown, PA, USA, for providing medical writing support, which was funded by Eisai Inc.

Disclosure

MA, JM, MJT, JW, SMG, TU, KN, and BAL are (or were at the time of the experiments) full-time employees of one of the following Eisai global network companies: Eisai Co., Ltd. (Japan), Eisai Inc. (USA), or Morphotek (USA). MHdB is a full-time employee of Oncodesign (France).

References

1 Jordan MA, Kamath K, Manna T, Okouneva T, Miller HP, Davis C, Littlefield BA and Wilson L: The primary antimitotic mechanism of action of the synthetic halichondrin E7389 is suppression of microtubule growth. Mol Cancer Ther *4*: 1086-1095, 2005.

2 Smith JA, Wilson L, Azarenko O, Zhu X, Lewis BM, Littlefield BA and Jordan MA: Eribulin binds at microtubule ends to a single site on tubulin to suppress dynamic instability. Biochemistry *49*: 1331-1337, 2010.

3 Doodhi H, Prota AE, Rodriguez-Garcia R, Xiao H, Custar DW, Bargsten K, Katrukha EA, Hilbert M, Hua S, Jiang K, Grigoriev I, Yang CP, Cox D, Horwitz SB, Kapitein LC, Akhmanova A and Steinmetz MO: Termination of protofilament elongation by eribulin induces lattice defects that promote microtubule catastrophes. Curr Biol *26*: 1713-1721, 2016.

4 Kuznetsov G, Towle MJ, Cheng H, Kawamura T, TenDyke K, Liu D, Kishi Y, Yu MJ and Littlefield BA: Induction of morphological and biochemical apoptosis following prolonged mitotic blockage by halichondrin B macrocyclic ketone analog E7389. Cancer Res *64*: 5760-5766, 2004.

5 Towle MJ, Salvato KA, Budrow J, Wels BF, Kuznetsov G, Aalfs KK, Welsh S, Zheng W, Seletsky BM, Palme MH, Habgood GJ, Singer LA, Dipietro LV, Wang Y, Chen JJ, Quincy DA, Davis A, Yoshimatsu K, Kishi Y, Yu MJ and Littlefield BA: *In vitro* and *in vivo* anticancer activities of synthetic macrocyclic ketone analogues of halichondrin B. Cancer Res *61*: 1013-1021, 2001.

6 Towle MJ, Salvato KA, Wels BF, Aalfs KK, Zheng W, Seletsky BM, Zhu X, Lewis BM, Kishi Y, Yu MJ and Littlefield BA: Eribulin induces irreversible mitotic blockade: implications of cell-based pharmacodynamics for *in vivo* efficacy under intermittent dosing conditions. Cancer Res *71*: 496-505, 2011.

7 Funahashi Y, Okamoto K, Adachi Y, Semba T, Uesugi M, Ozawa Y, Tohyama O, Uehara T, Kimura T, Watanabe H, Asano M, Kawano S, Tizon X, McCracken PJ, Matsui J, Aoshima K, Nomoto K and Oda Y: Eribulin mesylate reduces tumor microenvironment abnormality by vascular remodeling in preclinical human breast cancer models. Cancer Sci *105*: 1334-1342, 2014.

8 Yoshida T, Ozawa Y, Kimura T, Sato Y, Kuznetsov G, Xu S, Uesugi M, Agoulnik S, Taylor N, Funahashi Y and Matsui J: Eribulin mesilate suppresses experimental metastasis of breast cancer cells by reversing phenotype from epithelial-mesenchymal transition (EMT) to mesenchymal-epithelial transition (MET) states. Br J Cancer *110*: 1497-1505, 2014.

9 Towle MJ, Nomoto K, Asano M, Kishi Y, Yu MJ and Littlefield BA: Broad-spectrum preclinical antitumor activity of eribulin (Halaven®): Optimal effectiveness under intermittent dosing conditions. Anticancer Res *32*: 1611-1619, 2012.

10 Littlefield BA, Palme MH, Seletsky BM, Towle MJ, Yu MJ and Zheng W: Macrocyclic analogs and methods of their use and preparation. (Office USPaT ed). Alexandria, VA, USA, 2001. Patent no. US 6,214,865.

11 National Cancer Institute. Division of Cancer Treatment & Diagnosis: MDA-MB-435 and its derivation MDA-N, are melanoma cell lines, not breast cancer cell lines. Available at: https://dtp.cancer.gov/discovery_development/nci-60/mda-mb-435.htm. Accessed July 10, 2017.

12 Behrens BC, Hamilton TC, Masuda H, Grotzinger KR, Whang-Peng J, Louie KG, Knutsen T, McKoy WM, Young RC and Ozols RF: Characterization of a cis-diamminedichloroplatinum(II)-resistant human ovarian cancer cell line and its use in evaluation of platinum analogues. Cancer Res *47*: 414-418, 1987.

13 Bendell JC, Rodon J, Burris HA, de Jonge M, Verweij J, Birle D, Demanse D, De Buck SS, Ru QC, Peters M, Goldbrunner M and Baselga J: Phase I, dose-escalation study of BKM120, an oral pan-Class I PI3K inhibitor, in patients with advanced solid tumors. J Clin Oncol *30*: 282-290, 2012.

14 McGonigle S, Chen Z, Wu J, Chang P, Kolber-Simonds D, Ackermann K, Twine NC, Shie JL, Miu JT, Huang KC, Moniz GA and Nomoto K: E7449: A dual inhibitor of PARP1/2 and tankyrase1/2 inhibits growth of DNA repair deficient tumors and antagonizes WNT signaling. Oncotarget *6*: 41307-41323, 2015.

15 Kawano S, Asano M, Adachi Y and Matsui J: Antimitotic and non-mitotic effects of eribulin mesilate in soft-tissue sarcoma. Anticancer Res *36*: 1553-1561, 2016.

16 Kolb EA, Gorlick R, Reynolds CP, Kang MH, Carol H, Lock R, Keir ST, Maris JM, Billups CA, Desjardins C, Kurmasheva RT, Houghton PJ and Smith MA: Initial testing (stage 1) of eribulin, a novel tubulin binding agent, by the pediatric preclinical testing program. Pediatr Blood Cancer *60*: 1325-1332, 2013.

17 Cortes J, O'Shaughnessy J, Loesch D, Blum JL, Vahdat LT, Petrakova K, Chollet P, Manikas A, Diéras V, Delozier T, Vladimirov V, Cardoso F, Koh H, Bougnoux P, Dutcus CE, Seegobin S, Mir D, Meneses N, Wanders J, Twelves C and EMBRACE investigators: Eribulin monotherapy versus treatment of physician's choice in patients with metastatic breast cancer (EMBRACE): a phase 3 open-label randomised study. Lancet *377*: 914-923, 2011.

Received April 4, 2018
Revised May 14, 2018
Accepted May 17, 2018